NASA TECHNICAL NOTE

NASA TN D-4806

c.1

NASA TN D-4806

ULTRASONIC ATTENUATION IN SUPERCONDUCTING TANTALUM

by Zoltan W. Sarafi

Lewis Research Center

Cleveland, Ohio

NATIONAL AERONAUTICS AND SPACE ADMINISTRATION • WASHINGTON, D. C. • SEPTEMBER 1968

ULTRASONIC ATTENUATION IN SUPERCONDUCTING TANTALUM

By Zoltan W. Sarafi

Lewis Research Center
Cleveland, Ohio

NATIONAL AERONAUTICS AND SPACE ADMINISTRATION

For sale by the Clearinghouse for Federal Scientific and Technical Information
Springfield, Virginia 22151 – CFSTI price $3.00

ABSTRACT

Ultrasonic attenuation was measured in single crystals of tantalum at frequencies from 30 to 330 MHz. The crystals were oriented in the (100) and (110) directions. The attenuations of longitudinal and transverse waves were measured as a function of temperature and magnetic field. Curves are presented showing the transition between the normal and superconducting states. The zero-temperature energy gaps obtained were $3.3\ kT_c$ for both directions. The samples had ql values intermediate between those used by other investigators, and a comparison of results indicated that the energy gap in tantalum is lower for samples with larger electronic mean-free paths.

ULTRASONIC ATTENUATION IN SUPERCONDUCTING TANTALUM

by Zoltan W. Sarafi

Lewis Research Center

SUMMARY

Ultrasonic attenuation was measured in single crystals of tantalum at frequencies from 30 to 330 megahertz. The crystals were oriented in the (100) and (110) directions. The attenuations of longitudinal and transverse waves were measured as a function of temperature and magnetic field. Curves are presented showing the transition between the normal and superconducting states. The zero-temperature energy gaps obtained were $3.3\ kT_c$ (where k is the Boltzmann constant and T_c is the critical temperature) for both directions. The samples had $q\ell$ values (where q is the wave vector of the sound wave and ℓ is the mean-free path of conduction electrons) intermediate between those used by other investigators. A comparison of results indicated that the energy gap in tantalum is lower for samples with larger electronic mean-free paths.

INTRODUCTION

Bömmel (ref. 1) observed a rapid decrease in ultrasonic attenuation of lead and tin below their transition to the superconducting state at their critical temperatures T_c. Since the superconducting electrons cannot contribute to the energy absorption, his experiment indicated that detailed information of the coupling between conduction electrons and one lattice mode of vibration could be obtained by observation of the wave attenuation. Whereas direct measurements of conductivities yield information only on the integrated interactions including the entire vibration spectrum, ultrasonic measurements give the temperature dependence, anisotropy, and impurity influence of the energy gap that occurs in superconductors.

Ultrasonic attenuation measurements have been made on single crystals of tantalum. Levy, Rudnick, and Kagiwada (ref. 2 and 3) have investigated sound wave attenuation in two tantalum crystals for low $q\ell$ values (where q is the wave vector of the sound wave and ℓ is the mean-free path of conduction electrons). Their samples were oriented in the (110) direction. The temperature dependence of the attenuation coefficient, as well as

the energy gap, was obtained for both longitudinal and transverse waves polarized in the (001) direction. The zero-temperature energy gaps obtained were 3.4 and 3.5 kT_c. (All symbols are defined in the appendix.) Kagiwada (ref. 4) also investigated the temperature dependence of the attenuation coefficient and the energy gap in a single crystal of tantalum oriented in the (100) direction and used transverse waves at 45, 105, and 135 megahertz. The crystal had a longer mean-free path, and the claimed $q\ell$ values ranged from 0.5 to 1.8. A range of zero-temperature energy gaps was obtained between 3.06 and 3.12 kT_c.

The purpose of this investigation was to study tantalum single crystals with electronic mean-free-path lengths intermediate between those of Levy, Rudnick, and Kagiwada in the (110) samples and that of Kagiwada in the (100) sample to determine whether the difference in the measured energy gaps was caused by an anisotropy or whether the gap was a function of ℓ. In this investigation, transverse and longitudinal waves were used to measure the temperature dependence of the attenuation coefficient in both the (100) and (110) directions. The frequency range was 30 to 330 megahertz. The zero-temperature energy gaps and the temperature dependence of the gaps were determined for the two directions by using longitudinal waves on samples of comparable electronic mean-free paths.

EXPERIMENTAL PROCEDURE

The electrical equipment (fig. 1) used in this experiment was similar to that described by Morse (ref. 5) and by Chick, Anderson, and Truell (ref. 6). A synchronizer actuated a tuned-pulsed oscillator and a comparator pulse, alternately. The oscillator sent a sinusoidal voltage pulse of 10 to 330 megahertz for a 1- to 5 microsecond duration to the transducer, which was bonded to the sample. The resulting echoes were displayed on an oscilloscope. The change in height of an echo was then calibrated by comparing it to known attenuation values of a comparator pulse. The pulse comparator was a calibrated attenuator with a variable delay, and provided the comparator pulse that was triggered after each oscillator pulse. The comparator pulse was received by the same receiver as the echo pulse and could be displayed adjacent to any desired echo. The echo and comparator pulses were amplified by a 60-megahertz intermediate frequency strip that sent the signal to the oscilloscope. The oscilloscope in turn had a display scanner that gave an output to the Y-axis of an X, Y-recorder. The voltage on the Y-axis was proportional to the difference between the pulse height and a chosen zero level.

The piezoelectric transducers used in this experiment were tuned single crystals of quartz. The longitudinal waves were obtained from 10- and 30-megahertz fundamental frequency X-cut crystals. The transverse waves were obtained from orientation-marked

AC-cut crystals having a fundamental frequency of 10 megahertz. Both the single- and double-transducer techniques were used during the course of this work. The double-transducer technique was used to obtain high-frequency, transverse-wave attenuations in long samples. The single-transducer technique was used on all measurements of short samples. The transducers were bonded to clean surfaces with stopcock grease.

The sample was placed in a copper cylinder (ref. 7) that was in indirect contact with the helium bath. The temperature of the sample was varied from that of the bath by the joule heating of an 8000-ohm noninductively wound heater. The temperature was monitored with a germanium resistor calibrated to an error of ±0.003 K (points were every 0.250 K). The calibration points were used in an eighth-order polynomial of the form

$$\ln R = \sum_{n=0}^{8} A_n (\ln T)^n$$

where R is the resistance, A_n represents the coefficients that gave the best fit to the calibrated points, and T is the temperature. This form was used to generate pairs of temperature and resistance values in intervals of 0.005 K. Three 1/10-watt, 100-ohm carbon resistors electrically connected in parallel were calibrated against the germanium standard and then (because they were insensitive to the 0.2-T fields used in the study) were used to determine the effects of magnetic field on the attenuation. The voltage across the thermometers was amplified and then fed into the X-axis of the X, Y-recorder to obtain the temperature-dependent attenuation.

The magnetic field was obtained with a niobium-zirconium superconducting magnet, which was calibrated at 4.2 K with a Hall probe. Because of hysteresis in the magnet, the field uncertainty was ±0.0015 tesla. The superconducting magnet operated at the constant bath temperature to provide the longitudinal field. A signal proportional to the magnet current was obtained by a standard resistor used in series with the solenoid. The signal was applied to the X-axis of the recorder to obtain the field dependence of the attenuation during the superconducting to the normal transition at a fixed temperature.

The samples were 0.95 centimeter in diameter and oriented to within $1/2^{\circ}$ of the desired direction by the use of Laue reflection patterns. They were then spark cut to length. The crystal faces were lapped flat and made parallel to within 5×10^{-4} centimeter. The samples used were 1.246 to 0.451 centimeter long for the (100) crystals and 1.187 to 0.500 centimeter long for the (110) crystals.

RESULTS AND DISCUSSION

In this experiment, the transverse and longitudinal attenuations were recorded con-

tinuously by monitoring the echo height as a function of slowly varying temperature or magnetic field. The total attenuation measured resulted from electronic attenuation and other sources, such as lattice and impurity losses, acoustic losses from dispersion and reflections, and line losses. The line and acoustic losses (including those due to the transducer-sample bond) are not affected by a temperature change in the sample from 1.5 to 4.5 K (ref. 5). The change in lattice and impurity absorption, as well as the change in attenuation, due to normal electrons in this temperature range was determined by keeping the sample in the normal state with a magnetic field. The attenuation did not vary from its initial value at 4.5 K. The conclusion reached was that the lattice and the normal-state electronic contributions to the attenuation did not change significantly in this temperature range. The variation due to various input voltages of the attenuation between the normal and superconducting states was also checked to determine whether or not amplitude effects were as critical as those observed in lead by Love and Shaw (ref. 8). The observed variation with amplitude was small (0.04 dB/echo at 30 MHz) and was neglected. The large change in attenuation between the superconducting and normal states can only be caused by a change in the electronic attenuation. The change arises because superconducting electrons do not contribute to the attenuation, and, as more electrons become superconducting, the attenuation decreases. Since essentially all electrons become superconducting at $T \approx 0.35\ T_c$, the electronic contribution to the attenuation was obtained by measurement of the total change in attenuation from $T \geq T_c$ to a temperature of 1.54 K.

Pippard (ref. 9) gives the limits for the electronic attenuation as proportional to $l\nu^2/V$ for $ql < 1$ and to ν for $ql > 1$ (where ν is the frequency and V is the velocity of propagation). The frequency dependence of the electronic attenuation, which gives an indication of the ql value of the sample, is presented in figure 2 for longitudinal waves and in figure 3 for transverse waves. (The range of error is indicated in the figures.) Since the attenuation for all samples did not deviate from a frequency-squared relation, the conclusion was that they have values of $ql < 1$. Furthermore, the (110) sample had an experimentally determined electronic attenuation ratio $\alpha_{NT}/\alpha_{NL} = 9.79$ at 270 megahertz (where α_{NT} and α_{NL} are the electronic attenuations in the normal state for transverse and longitudinal waves of the same frequency). The Pippard ratio for $ql < 1$ (ref. 9) of $\alpha_{NT}/\alpha_{NL} = 3/4\ V_L^3/V_T^3$ has a predicted value of 9.78 (where V_L and V_T are the longitudinal and slow transverse velocities, respectively, for sound waves propagating in the (110) direction). The longitudinal and transverse velocities were calculated from the elastic constants measured at liquid-helium temperature by Featherston and Neighbours (ref. 10). The agreement in values would not be expected to hold for $ql > 1$.

Table I gives data on the crystals used in this study. The electronic attenuation was obtained from the slopes in figures 2 and 3 and is presented in terms of α_N/ν^2. This

number facilitates comparison of the samples in this study with those used by other investigators. A summary of the samples used by Levy, Rudnick, and Kagiwada (refs. 2 and 3) is given in the table along with ultrasonic data. For 270 megahertz, their two samples would have attenuations of 3.6 and 4.4 decibels per centimeter, respectively. Sample D had an attenuation of 7.15 decibels per centimeter at 270 megahertz. Since the electronic attenuation is proportional to $l\nu^2$ for $ql < 1$, the mean-free path of sample D is about 1.5 times that of their best sample. The sample used for the work by Kagiwada (ref. 4) is also given in table I. Since the ql of his sample was larger than 1, it had a larger value of l than that of sample D. So that the ultrasonic results can be compared with those obtained by other methods, the table is supplemented with the results obtained from tantalum crystals by various other experimental techniques.

A theoretical investigation by Bardeen, Cooper, and Shrieffer (BCS) (ref. 11) produced an expression for the ultrasonic attenuation as a function of temperature (the BCS theory of superconductivity). They used the fact that interactions between semifree electrons and phonons could result in paired electrons and thus account for an energy gap. They also used the coherence length of a pair of electrons and a modification of the density of electron states due to the gap to derive the equation for the relative attenuation of longitudinal waves in superconductors

$$\frac{\alpha_S}{\alpha_N} = 2f(\Delta) = \frac{2}{e^{\Delta/kT} + 1} \tag{1}$$

where α_S and α_N are the electronic attenuations in the superconducting and normal states, respectively, $f(\Delta)$ is the Fermi-Dirac function, and $2\Delta(T)$ is the energy gap at the Fermi surface. It was tacitly assumed in their treatment that the energy gap was isotropic around the Fermi surface and that $ql >> 1$. However, the expression was later shown to be valid for all values of ql (ref. 12).

The attentuations of longitudinal waves as a function of temperature in two samples are shown in figure 4. Propagation in the (100) direction in sample A is shown in figure 4(a). This sample had the highest transition temperature and the largest electronic mean-free path of the (100) samples, which is indicated by the electronic attenuation at T_c as a function of frequency (and shown in table I when the difference in velocities is considered). The solid line is the BCS theoretical curve. The data points near the solid line were obtained for a sound wave of 210 megahertz with no applied magnetic field. The electronic attentuation at T_c was 6.9 decibels per centimeter.

The influence of a constant magnetic field on the attenuation is also shown in fig ure 4(a). The dashed lines were obtained with background magnetic fields of 0.032 and 0.048 tesla. The procedure used to obtain these data involved cooling the sample in zero field, setting the field, and then slowly increasing the temperature. This procedure is

necessary to avoid the influence of trapped flux in the superconductor. The attenuation value obtained by cooling the sample in a field was higher than that obtained for a virgin sample. When the applied field was close to the upper critical field $H_{c2}(T)$, the attenuation had a change in slope that was consistent with observed attenuation (ref. 4) in the mixed state of a type II superconductor.

The variation of attenuation with temperature for longitudinal waves propagating in the (110) direction is shown in figure 4(b). The curve is essentially the same as that obtained for the (100) sample. The experimental data used in figure 4 were also used to obtain the energy gaps.

Transverse waves in superconductors have been treated theoretically. Morse and Claiborne (refs. 13 and 14) made calculations in the transition region at temperatures near T_c. Their theory predicts a drop in relative attenuation, as T is reduced below T_c, followed by a residual attenuation given by

$$\frac{\alpha_{ST}}{\alpha_{NT}} = 2gf(\Delta) \tag{2}$$

where

$$g = \frac{3}{2(q\ell)^2}\left[\left(\frac{1 + (q\ell)^2}{q}\right)\tan^{-1}\nu q - 1\right]$$

The variation of the electronic attenuation with temperature is presented in figure 5. There was no sharp drop as observed in type I superconductors (ref. 13), but in each case a BCS-type falloff (eq. (1)) starting from T_c was observed. The Pippard coefficient g in equation (2) is approximately 1 for these samples. (Type I and II superconductors are discussed in many texts, e.g., ref. 15.) The solid line in figure 5 was calculated from equation (1), which is the limit of equation (2) for $q\ell = 0$. The dashed line in figure 5(a) was obtained from equation (2) for $q\ell = 1$, which gives a value of 0.87 for g. A factor of 1 for g would be expected for $q\ell < 0.5$. The absence of a sharp drop in the attenuation at T_c for shear waves has been observed in tantalum by Levy, Rudnick, and Kagiwada (refs. 2 and 3). If a bulk sample with large values of $q\ell$ could be obtained, the sharp drop in attenuation might be observed in tantalum.

Since the tantalum Fermi surface is not a sphere (ref. 16), there may be anisotropy in the energy gap. The samples used in this study have intermediate $q\ell$ values, and two processes contribute to the attenuation. In the case of $q\ell \gg 1$, the electrons that contribute to attenuation of longitudinal waves are those with a velocity component in the direction of wave propagation equal in magnitude to the sound velocity. This requirement

limits the interacting electrons to thin rings around the Fermi surface. In the case of $q\ell \ll 1$, essentially all electrons around the Fermi surface contribute to the attenuation. The total anisotropy of the energy gap can be measured only in samples with values of $q\ell \gg 1$. In this study of samples with intermediate $q\ell$ values, both attenuation processes took place, and the full anisotropy could not be determined.

The (100) and (110) orientations were used to study the energy gap. The calculations of the zero-temperature energy gaps were obtained from figure 6. Figures 6(a) and (b) are curves obtained from the data used in figures 4(a) and (b) and equation (1). The slope of the curve at $T/T_c = 0$ is $kT_c/\Delta(O)$. The gaps obtained were essentially equal with values of 3.32 ± 0.10 and $3.34 \pm 0.12\ kT_c$ for the (100) and (110) directions, respectively. The value obtained for the (100) sample was high in comparison with $3.1\ kT_c$ reported by Kagiwada (ref. 4) and the value for the (110) sample was low in comparison with the $3.5\ kT_c$ reported by Levy, Kagiwada, and Rudnick. Since the samples had values of $q\ell < 1$, a definite determination of the gap anisotropy could not be made. However, the gap is apparently affected by the mean-free path of the electron. The trend indicates that larger $q\ell$ values reduce the gap from the BCS value of $3.5\ kT_c$.

Figure 7 gives the energy gap dependence as a function of temperature. The solid line is the BCS curve for the energy gap with $2\Delta(O) = 3.5\ kT_c$. The data points were obtained from the experimental values of α_S/α_N given in figure 4 and the plot of $kT/\Delta(O) \ln (2\alpha_N/\alpha_S - 1) = \Delta(T)/\Delta(O)$ as a function of T/T_c. The zero-temperature energy gaps used were the values of $\Delta(O)$ obtained in figure 6.

The upper critical magnetic field H_{c2} was determined ultrasonically by finding the field that corresponded to the intersection of the normal and superconducting attenuations at preset temperatures. Figures 8(a) and (b) are plots of these critical fields as a function of $1 - (T^2/T_c^2)$ for the (100) and (110) samples, respectively.

The hysteresis effect mentioned in the discussion of figure 4(a) was observed when the field was raised to drive the sample normal and then decreased. Reversing the field polarity and repeating the process resulted in the formation of the butterfly-shaped pattern in figure 9. In all runs, the samples were initially heated, the previous background field was removed, and then the samples were cooled from the normal to the superconducting state before the field was again established. The field at which flux enters the sample H_{ce} is also represented in figure 8. This field was determined by the intersection of slopes in the butterfly curves where the superconducting attenuation increased from its initial value at each temperature. The extrapolated values of $H_{c2}(O)$ of 0.091 and 0.090 tesla obtained for the (100) and (110) samples, respectively, were higher than Budnick's values (ref. 17). This difference, also observed by Levy and Rudnick (ref. 2), indicates that the samples are not as pure as those of Budnick's.

CONCLUDING REMARKS

Ultrasonic attenuation was observed for frequencies from 30 to 330 megahertz in five single crystals of tantalum. The crystals were oriented in the (100) or (110) directions. Both polarization directions for transverse, as well as longitudinal, waves were studied. The attenuation was measured as a function of temperature and magnetic field.

The samples had a total normal attenuation proportional to ν^2 for all frequencies tested, which implies that the samples were in the range of $q\ell < 1$. This conclusion was further substantiated by the fact that the transverse wave attenuation followed the BCS curve from the transition temperature. The samples used, which exhibited characteristics of type II superconductors, did not show the sharp fall for transverse waves observed in type I superconductors. Since the residual attenuation is given by $\alpha_{ST}/\alpha_{NT} = g(q\ell)2f(\Delta)$, the Pippard coefficient g is nearly 1 for these samples.

The energy gap was obtained from longitudinal waves studied for both crystal orientations. The gap obtained was $2\Delta(O) = 3.32 \pm 0.10$ and $3.34 \pm 0.12\ kT_c$ for the (100) and (110) directions, respectively. Essentially no anisotropy was observed, but this does not imply that there would be no anisotropy in samples with values of $q\ell \gg 1$. The gap is intermediate between the 3.5 and $3.1\ kT_c$ values obtained by other investigators. The differences indicate that the energy gap in tantalum is smaller for samples of larger electronic mean-free paths.

The effect of the magnetic field on the transition was observed. A graphical comparison of the attenuations with and without a magnetic field was made. Hysteresis in the attenuation as a function of field was observed in the intermediate state of the type II superconductors. The critical fields H_{ce} and H_{c2} were obtained by the ultrasonic monitoring of transitions into the intermediate state.

Lewis Research Center,
National Aeronautics and Space Administration,
Cleveland, Ohio, June 21, 1968,
129-02-05-11-22.

APPENDIX - SYMBOLS

$f(\Delta)$	Fermi-Dirac function = $1/\left[\exp(\Delta/kT) + 1\right]$
g	Pippard transverse coefficient (eq. (2))
H	magnetic field, T
H_{ce}	critical field at which flux enters sample, T
H_{c2}	upper critical magnetic field, T
k	Boltzmann constant
l	mean-free-path length of conduction electrons, cm
P	polarization orientation vector
q	sound wave vector
T	temperature, K
$\Delta(T)$	energy gap parameter
T_c	critical temperature, K
V	velocity of propagation of sound
V_L	wave velocity in longitudinal direction
V_T	wave velocity in transverse direction
α_N	electronic attenuation of wave in normal state
α_{NL}	electronic attenuation in normal state of longitudinal wave
α_{NT}	electronic attenuation in normal state of transverse wave
α_S	electronic attenuation of wave in superconducting state
ν	frequency, MHz

REFERENCES

1. Bommel, H. E.: Ultrasonic Attenuation in Superconducting Lead. Phys. Rev., vol. 96, no. 1, Oct. 1, 1954, pp. 220-221.

2. Levy, Moises; and Rudnick, Isadore: Ultrasonic Determination of the Superconducting Energy Gap in Tantalum. Phys. Rev., vol. 132, no. 3, Nov. 1, 1963, pp. 1073-1080.

3. Levy, Moises; Kagiwada, Reynold; and Rudnick, Isadore: Ultrasonic Attenuation of Transverse Waves in V, Nb, and Ta for $q\ell < 1$. Phys. Rev., vol. 132, no. 5, Dec. 1, 1963, pp. 2039-2046.

4. Kagiwada, Reynold S.: Ultrasonic and Thermal Effects in Superconductors. Tech. Rep. 26, Univ. California, Los Angeles, Dec. 1966. (Available from DDC as AD-644182.)

5. Morse, R. W.: Ultrasonic Attenuation in Metals at Low Temperatures. Progress in Cryogenics. Vol. 1, K. Mendelssohn, ed., Heywood and Co., Ltd., 1959, pp. 219-259.

6. Chick, Bruce; Anderson, George; and Truell, Rohn: Ultrasonic Attenuation Unit and and Its use in Measuring Attenuation in Alkali Halides. J. Acoust. Soc. Am., vol. 32, no. 2, Feb. 1960, pp. 186-193.

7. Simmons, Joseph H.: Ultrasonic Attenuation in Superconducting Niobium. NASA TN D-3817, 1967.

8. Love, R. E.; and Shaw, R. W.: Ultrasonic Attenuation in Superconducting Lead. Rev. Mod. Phys., vol. 36, pt. 1, Jan. 1964, pp. 260-263.

9. Pippard, A. B.: Ultrasonic Attenuation in Metals. Phil. Mag., vol. 46, no. 381, Oct. 1955, pp. 1104-1114.

10. Featherston, F. H.; and Neighbours, J. R.: Elastic Constants of Tantalum from 4.2° K to 300° K. Bull. Am. Phys. Soc., vol. 7, no. 3, Mar. 1962, p. 236.

11. Bardeen, J.; Cooper, L. N.; and Schrieffer, J. R.: Theory of Superconductivity. Phys. Rev., vol. 108, no. 5, Dec. 1, 1957, pp. 1175-1204.

12. Tsuneto, T.: Ultrasonic Attenuation in Superconductors. Phys. Rev., vol. 121, no. 2, Jan. 15, 1961, pp. 402-415.

13. Morse, R. W.: Ultrasonic Attenuation in Superconductors. IBM J. Res. Dev., vol. 6, no. 1, Jan. 1962, pp. 58-62.

14. Claiborne, Lewis T., Jr.; and Morse, Robert W.: Study of the Attenuation of Ultrasonic Shear Waves in Superconducting Aluminum. Phys. Rev., vol. 136, no. 4A, Nov. 16, 1964, pp. A893-A905.

15. Lynton, Ernest A.: Superconductivity. John Wiley and Sons, Inc., 1962.

16. Fawcett, E.; Reed, W. A.; and Soden, R. R.: High-Field Galvanomagnetic Properties of Niobium and Tantalum. Phys. Rev., vol. 159, no. 3, July 15, 1967, pp. 533-539.

17. Budnick, J. I.: Some Studies of the Superconducting Transition in Purified Tantalum. Phys. Rev., vol. 119, no. 5, Sept. 1, 1960, pp. 1578-1586.

18. Richards, P. L.; and Tinkham, M.: Far-Infrared Energy Gap Measurements in Bulk Superconducting In, Sb, Hg, Ta, V, Pb, and Nb. Phys. Rev., vol. 119, no. 2, July 15, 1960, pp. 575-590.

19. Giaever, Ivar: Energy Gaps in Some Hard Superconductors. Low Temperature Physics. R. O. Davies, ed., Butterworth Publ., Inc., 1963, pp. 171-172.

20. Connolly, A.; and Mendelssohn, K.: Thermal Conductivity of Tantalum and Niobium below 1^{O} K. Proc. Roy. Soc., ser. A, vol. 266, no. 1327, Mar. 27, 1962, pp. 429-439.

21. Roberts, B. W.: Superconducting Materials and Some of Their Properties. Rep. 63-RL-3252M, General Electric Co., Mar. 1963.

TABLE I. - TANTALUM DATA

(a) Acoustic results of present investigation

Sample	Crystal orientation	Sample length, cm	Critical temperature, T_c, K	Zero-temperature energy gap, $2\Delta(0)$, kT_c	Frequency, ν, MHz	Upper critical magnetic field, H_{c2}, T	Electronic attenuation parameter, α_N/ν^2, (dB)(sec^2)/cm	Wave	Direction of polarization, P
A	(100)	1.246	4.46	3.3±0.1	210	0.091	1.59×10^{-16}	Longitudinal	----
B	(100)	.451	4.37	-------	---	-----	3.56	Transverse	(001)
C	(110)	1.187	4.44	-------	---	-----	1.30	Longitudinal	----
D	(110)	.629	4.39	3.3±0.1	270	.090	9.54	Transverse	(1$\bar{1}$0)
E	(110)	.500	4.39	-------	---	-----	3.16	Transverse	(001)

(b) Acoustic results of other investigations

Investigator	Reference	Sample	Crystal orientation	Sample length, cm	Critical temperature, T_c, K	Zero-temperature energy gap, $2\Delta(0)$, kT_c	Frequency ν, MHz	Upper critical magnetic field, H_{c2}, T	Electronic attenuation parameter, α_N/ν^2, (dB)(sec^2)/cm	Wave	Direction of polarization, P	Resistivity ratio
Levy and Rudnik	2	I	(110)	2.680	4.36	3.4±0.2	---	-----	0.5×10^{-16}	Longitudinal	----	35
		II	(110)	2.78	4.42	3.5±0.2	---	0.120	.6	Longitudinal	----	40
Levy, Rudnik, and Kagiwada	3	Three samples	(110)	-----	----	3.5±0.2	---	-----	2.6×10^{-16}	Transverse	(001)	---
Kagiwada	4	3	(100)	0.95	4.48	3.06±0.05 3.08±0.05 3.12±0.05	45 105 135	0.085	---------	Transverse	----	450

(c) Results of other methods

Reference	Method	Critical temperature, T_c, K	Zero-temperature energy gap, $2\Delta(0)$, kT_c	Critical magnetic field, H_c, T
Richards and Tinkham (ref. 18)	Infrared absorption	----------	3.0	----------
Giaever (ref. 19)	Tunneling	----------	3.5	----------
Connolly and Mendelssohn (ref. 20)	Thermal conductivity	----------	3.5	----------
Budnick (ref. 17)	Resistance measurements	4.457 to 4.482	---	0.0821 to 0.0846
Roberts (ref. 21)	Magnetic	4.483	---	0.0830
	Calorimetric	4.39	---	0.0780

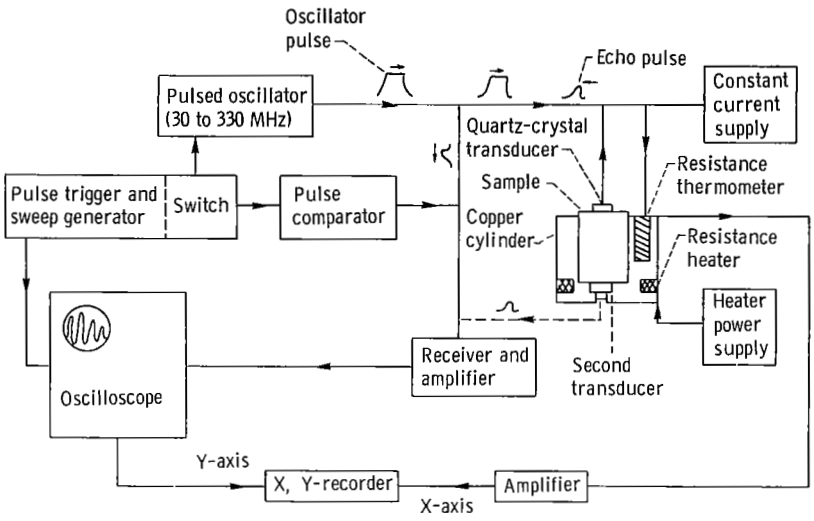

Figure 1. - Block diagram of equipment used to observe attenuation in tantalum.

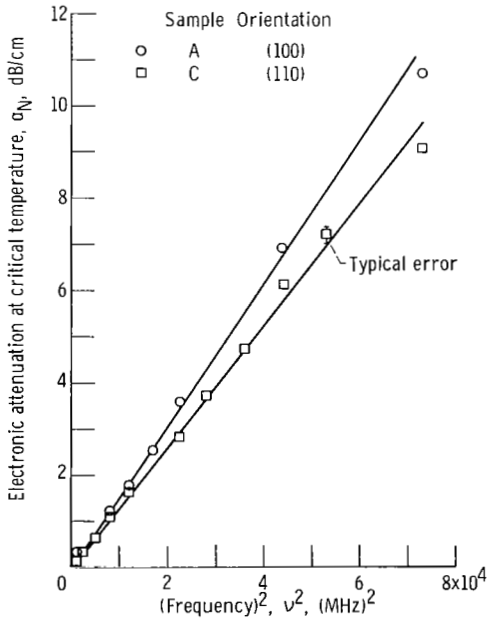

Figure 2. - Dependence of electronic attenuation on frequency for longitudinal waves.

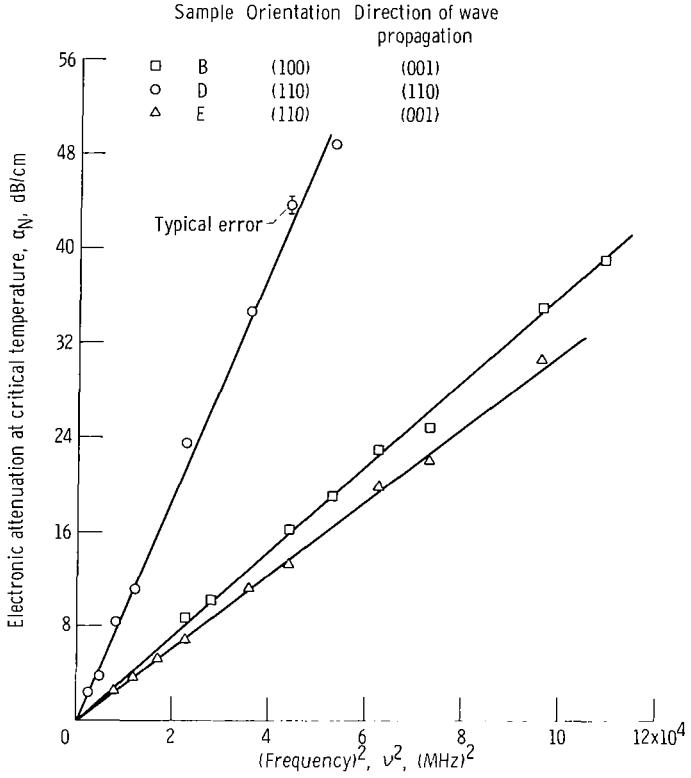

Figure 3. - Dependence of electronic attenuation on frequency for transverse waves.

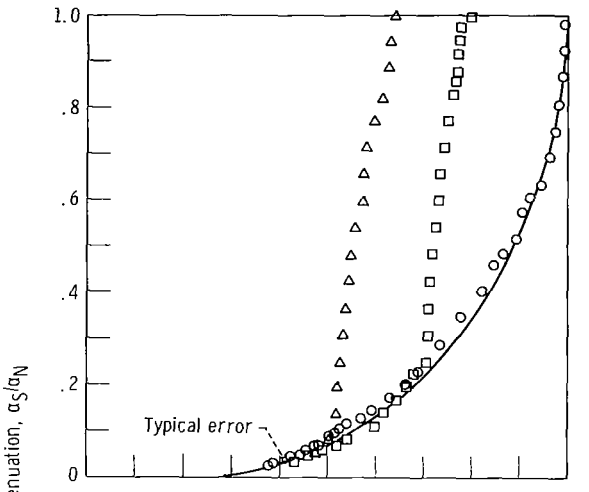

(a) Propagation in sample A along (100) direction. Frequency, 210 megahertz; electronic attenuation of wave in normal state, 6.9 decibels per centimeter.

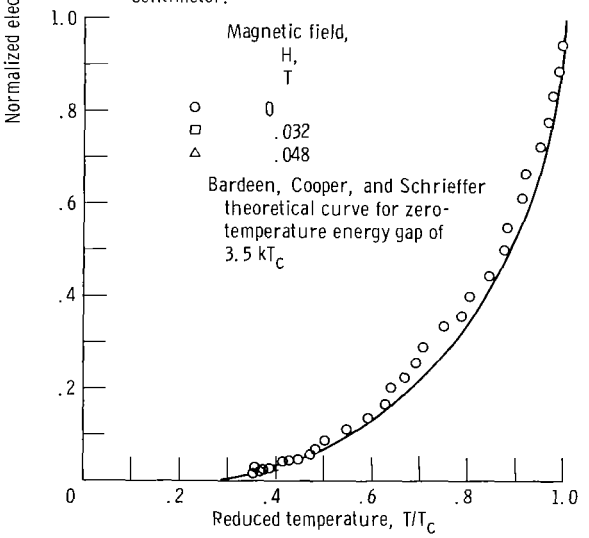

(b) Propagation in sample D along (110) direction. Frequency, 270 megahertz; electronic attenuation of wave in normal state, 7.15 decibels per centimeter.

Figure 4. - Variation of electronic attenuation in superconducting state for longitudinal waves.

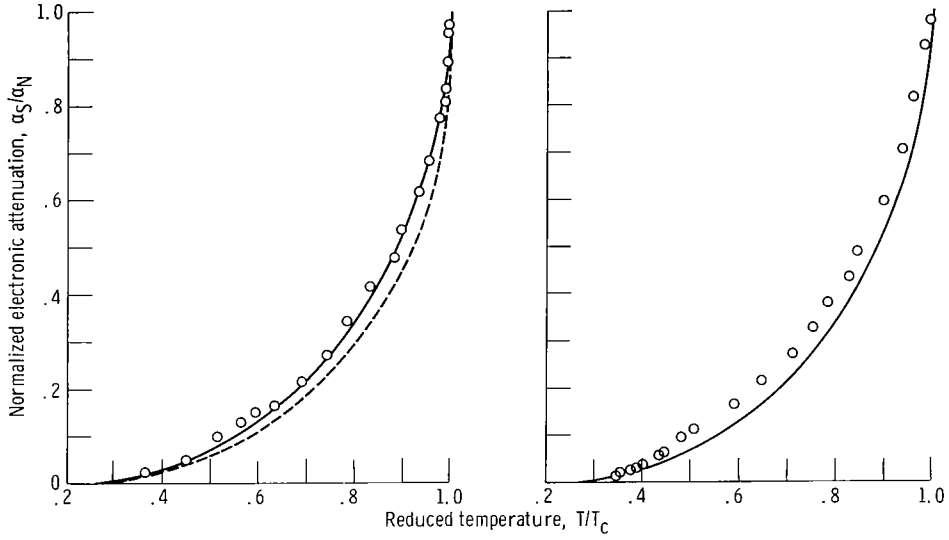

(a) Propagation in (110) direction in sample D with polarization along (110) direction. Frequency, 150 megahertz; electronic attenuation of wave in normal state, 22.3 decibels per centimeter.

(b) Propagation in (100) direction in sample B with polarization along (001) direction. Frequency, 170 megahertz; electronic attenuation of wave in normal state, 10.3 decibels per centimeter.

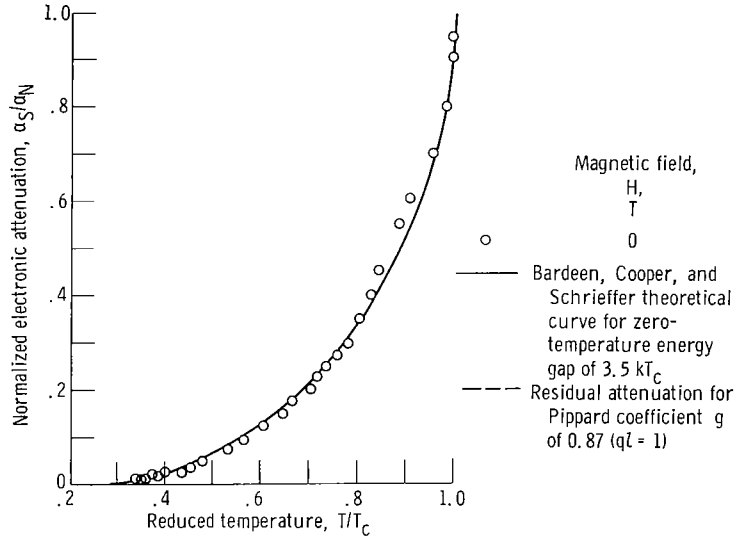

(c) Propagation in (100) direction in sample E with polarization along (001) direction. Frequency, 250 megahertz; electronic attenuation of wave in normal state, 19.9 decibels per centimeter.

Figure 5. - Variation of electronic attenuation in superconducting state for transverse waves.

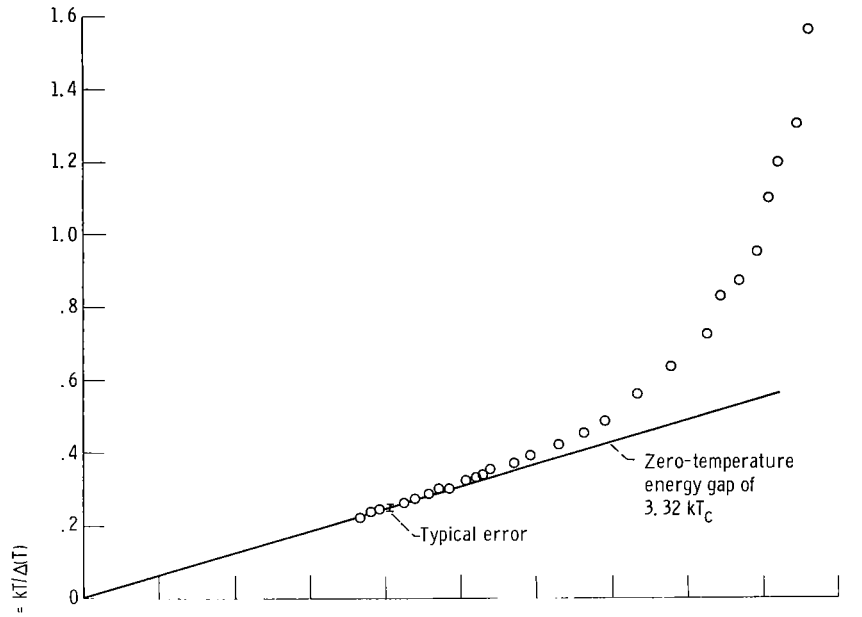

(a) Propagation along (100) direction in sample A at frequency of 210 megahertz.

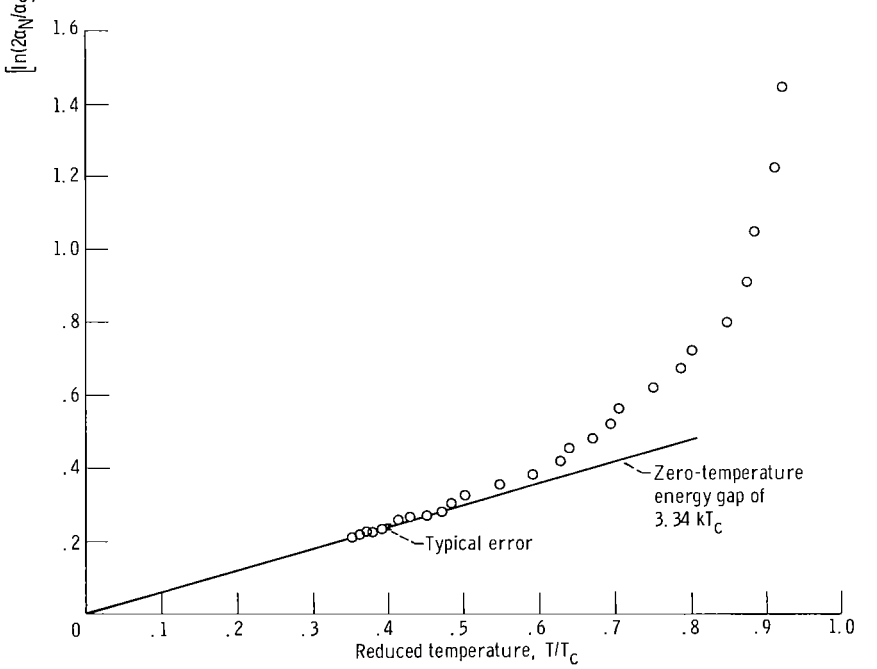

(b) Propagation along (110) direction in sample D at frequency of 270 megahertz.

Figure 6. - Calculation of zero-temperature energy gap.

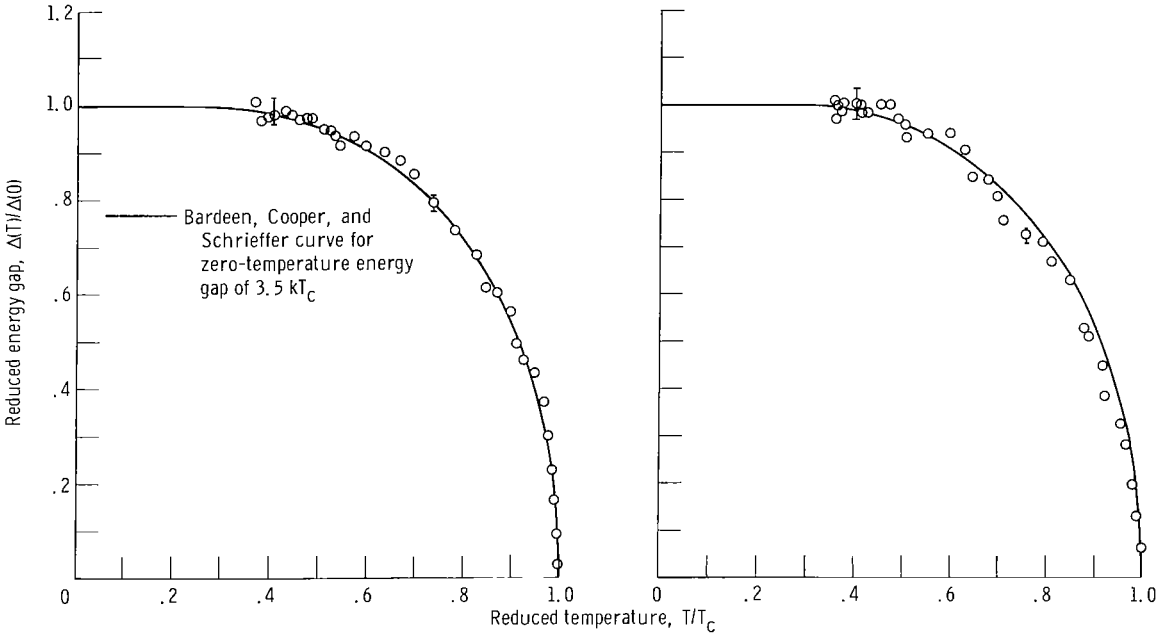

(a) Propagation along (100) direction in sample A for zero-temperature energy gap of 3.32 kT$_c$.

(b) Propagation along (110) direction in sample D for zero-temperature energy gap of 3.34 kT$_c$.

Figure 7. - Energy gap dependence on temperature for longitudinal waves.

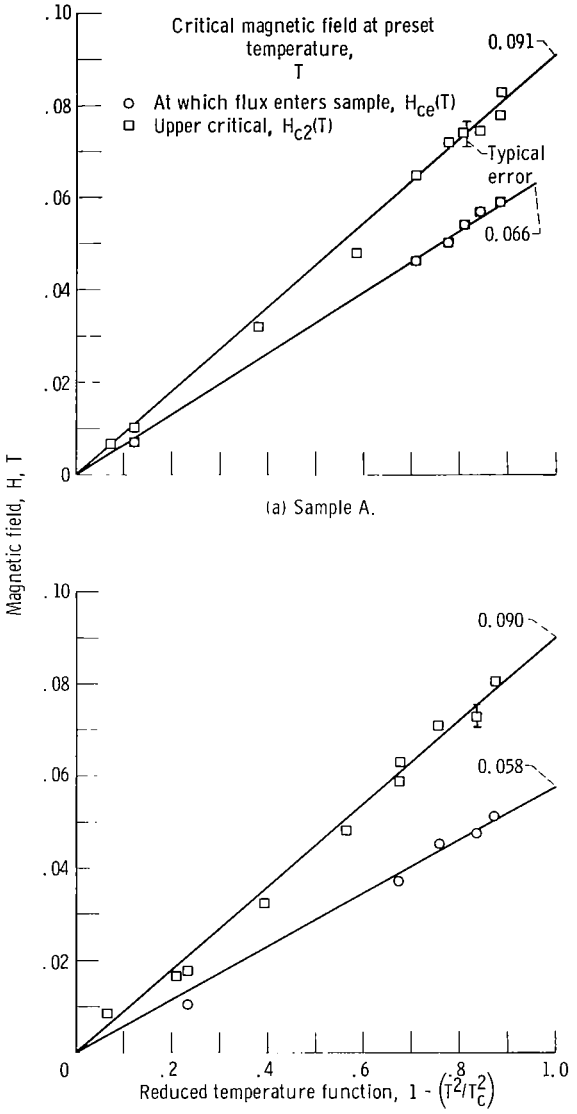

Figure 8. - Critical magnetic field as function of temperature.

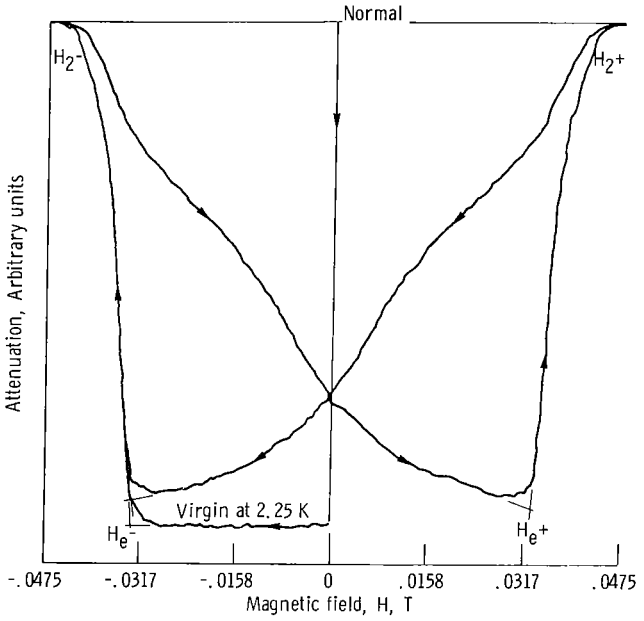

Figure 9. - Butterfly pattern formed as result of monitoring echo height as function of magnetic field at fixed temperature of 2.25 K for sample A. Upper critical magnetic field, 0.046 tesla; critical field at which flux enters sample, 0.033 tesla.

NASA-Langley, 1968 —— 26 E-4466